Visions and Strategies for Reinforcing Additively Manufactured Concrete Structures Reinforcing Materials
https://doi.org/10.52825/ocp.v1i.80

Submitted: 5 Oct. 2021 | Accepted: 29 Nov. 2021 | Published: 15 Feb. 2022

Simultaneous Integration of Continuous Mineral-bonded Carbon Reinforcement into Additive Manufacturing with Concrete

Tobias Neef[1] [https://orcid.org/0000-0002-8256-1455] and Viktor Mechtcherine[1] [https://orcid.org/0000-0002-4685-7064]

[1]Technische Universität Dresden, Germany

Abstract. 3D concrete printing is becoming more and more popular, not only in research but also in practice of construction. One of the main challenges however remains the integration of reinforcement. This publication focuses on the use of continuous fibers for this purpose. The special feature of the new type of carbon yarns applied is the mineral impregnation used instead of the conventional polymer one. Such reinforcement not only yields excellent mechanical properties, but also offers many advantages, specifically with respect to processing flexibility and is therefore very well suited for additive manufacturing. The concrete for 3D printing to be reinforced with such yarns must meet particular requirements, especially when the finest concrete filaments are printed. This is also a subject of the article at hand.

Keywords: Digital construction, digital concrete, Additive Manufacturing, 3D concrete printing, reinforcement, mineral-bonded carbon fibre

Conference presentation video: https://doi.org/10.5446/56113

Introduction

The additive manufacturing with concrete, also often called 3D concrete printing (3DCP), offers a number of advantages such as saving manpower, time and resources and thus also reducing CO_2 footprint of concrete construction [1]. The work processes are simulated and optimized in advance on a digital construction site. This is followed by implementation on the real construction site [2] or the production of prefabricated parts in a factory, which only need to be assembled on site. An example for that is the bicycle bridge in the Netherlands [3], where components were first printed in a factory and then connected to form a bridge with pre-stressed reinforcement. Formwork-free construction opens up new shape-free design possibilities, especially curves or wave shapes, as can be seen on the individual segments of the bridge.

While 3DCP develops fast towards applications in the practice of construction, the integration of reinforcement into these technologies still presents a challenge. There are a number of options with respect to materials to be used, ranging from conventional steel reinforcement [4] to short-fiber reinforcement [5], carbon reinforcement [6] or prestressed reinforcement [3]. The different variants were widely discussed in Mechtcherine et al. [7]. In this article, the focus will be on simultaneous and continuous carbon fiber reinforcement. The special feature here is that the carbon is impregnated not with a polymer, following the established technique for carbon reinforcement, but with a mineral suspension.

Mineral-bonded carbon reinforcement

Why do we use mineral impregnated fiber reinforcement?

Mineral-impregnated carbon yarns have several advantages over polymer-impregnated fiber reinforcements. The easy formability of the freshly impregnated yarn is of a particular importance for additive manufacturing applications. The yarn can be deposited in any geometry without strain, thus exploiting the full potential of the geometric freedom of 3D printing. The carbon reinforced concrete filaments can be deposited in fine and narrow paths with a small cross-section, since the carbon reinforcement requires only a very thin concrete cover. This allows the reinforcement to be integrated into the border areas of the components in a statically favorable manner. A thin cover leads to material savings and thus more environmentally friendly construction. Furthermore, the mineral impregnation shows a significantly higher temperature resistance [8] than polymeric impregnation materials and enables a very intensive bond between reinforcement and concrete. At 200 degrees, the pullout force was double [8]. Concrete components with mineral-impregnated reinforcement therefore exhibit a very finely distributed crack pattern with small crack widths when subject to bending or tensile loads. This reduces possible ingress of agrecive substances into the composite, which is beneficial to its durability.

Composition and properties of the mineral impregnation suspension

To prepare the mineral impregnation suspension, two ultrafine cements (Mikrodur R-X, Mikrodur P-U, Dyckerhoff Germany) and a microsilica suspension (EMSAC 500 SE, BASF Germany) with superplasticizer are suspended in water. 95% of all particles by weight have sizes smaller than 9 µm, so that most particles can penetrate between the carbon filaments with diameters of about 7 µm after excitation. Figure 1a shows the grading curves of the constituents of the suspension in comparison to a typical CEM I 52.5 R cement. Figure 1b shows a carbon filament with adhering suspension particles. The water-to-binder ratio of the suspension is 0.8. The viscosity is adjusted using superplasticizer "MSH flüssig" to a run-out time in the Marsh Funnel of approximately 30 seconds.

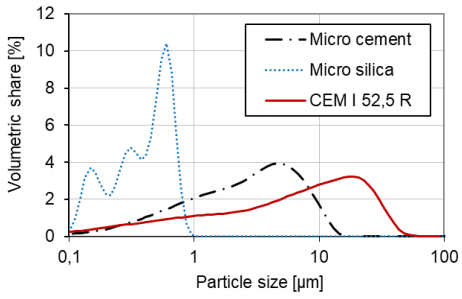

(a)

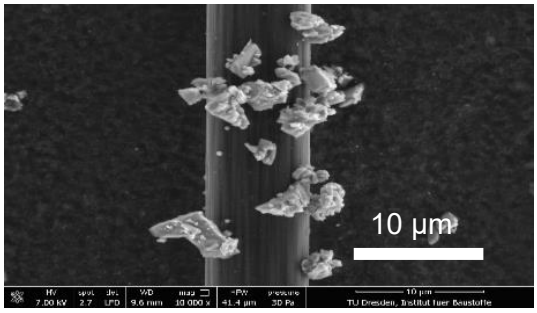

(b)

Figure 1. (a) Particle size distributions of mineral suspension and (b) micrograph of carbon fiber with adhering micro-cement with D95 < 9 µm [9].

A carbon yarn SIGRAFIL® C T50-4.4/255-E100 (SGL) was used as continuous reinforcement fiber. The yarn consists of 50,000 individual filaments with epoxy resin sizing. Complete impregnation of yarn is effectuated by multiple deflection of the yarn in the suspension. To ensure the cohesion of the filaments in the freshly impregnated yarn, the carbon yarn is spirally wrapped with a cotton thread. The carbon yarn is then wound onto a spool and fed into the additive manufacturing process. The spooled yarn can be processed for about four hours. The manufacturing process is only outlined here. A detailed description is given in Mechtcherine et al. [9].

The carbon percentage in the impregnated yarn after hardening is approximately 30 % by volume. The average diameter of a mineral-impregnated roving is approx. 3.1 mm and the corresponding cross-sectional area approximately 7.5 mm². The failure force in the uniaxial tension test (mean value) is 4.56 kN. This corresponds to a tensile strength of 581 MPa based on the total cross-section of the impregnated yarn and 2,271 MPa based on the cross-sectional area of all carbon filaments in the yarn (1.92 mm²). The modulus of elasticity related to the carbon cross-sectional area averages 249.4 GPa and is thus close to the modulus of elasticity of the carbon yarn (250 GPa).

Integration between or into concrete filaments

The additive manufacturing itself is performed with a gantry printer. The lab-scale device offers a printing space of 1.3 m x 1.3 m x 1.0 m. During production, the mixed concrete is held in a hopper. From this, the concrete is conveyed to the nozzle via an eccentric screw pump. Then it is extruded into the desired shape. There are two basic methods for integrating carbon reinforcement into the existing additive manufacturing process:

- Contiguous process: Extrusion of a concrete filament followed by deposition of the carbon rovings onto it and subsequent covering of the reinforcement yarn by extrusion of the next concrete filament [10]. The advantage of this method is that the placement of concrete and reinforcement are decoupled in time. Thus, the number of deposited reinforcements be-tween the concrete filaments can be varied according to the expected local loading. This reduces the cost of reinforcement and promotes environmentally friendly and resource-saving construction. Disadvantages are the higher time requirement if the layers are passed over twice or more times on one hand. On the other hand, the placement of the reinforcement in the joint between two concrete filaments additionally weakens this porous region. Finally, transverse tensile stresses resulting from the bond between yarn and concrete can lead to splitting along the bonded joint; see Figure 2a.
- Simultaneous process: The carbon reinforcement is embedded in the concrete filament and deposited with it. The advantages of this method are complete encasement of the yarn without weakening the joint in an efficient and time-saving manner. The disadvantage is a lacking option of having crossings and overlaps of reinforcement layers which can be favorable for transfer of forces in a print element. Note that for a simultaneous process, the degree of reinforcement in the concrete filament can be adapted using a special nozzle geometry ProfiCarb, in which up to six carbon rovings can be integrated simultaneously [6].

(a) (b)

Figure 2. Fracture pattern of a specimen produced (a) in the contiguous process, and (b) in the simultaneous process.

First studies and results

Uniaxial tension test on printed and cast specimens

In this section, results of investigations on specimens from both the simultaneous process and the conventional casting are presented. Some of the results have already been published in the journal Beton- und Stahlbetonbau [6].

For the tests, a fine-grain concrete was chosen which is often used for 3D printing processes at the Institute for Construction Materials at the TU Dresden; see e.g. [11], [12]. Portland cement, microsilica slurry and fly ash were used as binders. The maximum grain size of the aggregate was 2 mm. The composition is given in Table 1.

Table 1. Composition of printable fine-grained concrete under investigation.

Constituent	Supplier / product name	[kg/m³]
Cement CEM I 52.5 R ft	Opterra	392
Fly ash SFA	Steament H4	214
Microsilica	EMSAC 500 SE, BASF	214
Sand 0.06-0.2	BCS 413	253
Sand 0-1	Ottendorf	253
Sand 0-2	Ottendorf	759
Water	Tab water	139
Superplasticizer	Sky 593, BASF	11

To compare the mechanical performance of the specimens from the two types of production, specimens for uniaxial tension tests were produced and loaded to failure. Both the printed and the conventionally cast specimens had a length of 300 mm and a cross-section of approximately W x H = 20 mm x 40 mm. The reinforcement was arranged in the center of the cross-section at a height of 10 mm. The reinforcement consisted of three mineral-impregnated car-bon yarns placed at 10 mm distance to each other.

The two types of specimens were prepared almost simultaneously. First, the specimens were prepared using the simultaneous printing process, as shown in Figure 3. Then, additional concrete was extruded into a container and cast into a mold. The mold was first filled with concrete up to half its height; then the reinforcement was removed from the roll, put onto concrete and tightened; finally, further concrete was filled on top of it. The production of these specimens using extruded concrete was necessary since the consistency of concrete changes significantly due to the extrusion and the associated energy input. The specimens produced by the printing were complemented with load introduction regions at their ends at the specimen age of two days. Each such region had a length of 200 mm and a width of 100 mm and was grouted with self-compacting concrete. In the conventionally cast specimens, the load application area is already given by the shape of the mold; see Figure 3. Before testing, the load application regions of all specimens were ground to a thickness of 20 mm to avoid stress peaks during clamping in the Instron 8501 testing machine. The tension test was performed with a displacement rate of the crosshead of 1 mm/min until breakage. Figure 4a shows a stress-strain diagram with the results of the uniaxial tension tests.

Figure 3. Left: expansion specimen printed at the top and molded at the bottom. Right: printing process.

The conventionally produced strain plates have a higher average yarn strength of 2.078 GPa attained at 12.6‰ strain, while the scatters of strain capacity and tensile strength are greater than those recorded for the printed specimens; which yielded an average yarn strength of 1.578 GPa at a strain of 10.9‰. The reason for this difference is probably the quality of the embedment into concrete. Defects such as air inclusions can occur during or under extrusion due to insufficient conveying of material. Thus, the force transmission from the carbon yarns into concrete is disturbed. Furthermore, while the reinforcement in the conventionally produced specimens is exactly centered and stretched, this is not always the case within the printed specimens using the online process; see also cross-section analyses in the next section.

The crack initiation and crack growth were photogrammetrically recorded using a GOM ARAMIS measurement system. For this purpose, the smooth underside of the strain plate was equipped with a stochastic speckle pattern. During tension test this specimen surface was recorded at a frame rate of 1/s. In the image analysis, five distance gauges were placed equidistantly over each crack formed. The mean value of the distance gauges indicates the crack width used for further evaluation. The distance measurement between the cracks was made along the center axis of the specimens. In addition, the strain in the measurement area was determined using two virtual extensometers, which were placed close to the right and left sides of the specimen. For the evaluation, all crack widths were considered at 50% and 90% of the ultimate strain. The determined crack widths were assigned to crack classes of 0.1 mm width (example: crack class 0.2 mm contains cracks with widths > 0.1 mm and ≤ 0.2 mm). By relating the number of cracks in the measuring range to the length of the measuring range, a crack density (unit: cracks/m) can be calculated. In Figure 4b, the elements of a crack class were determined for all specimens of a production variant and converted into a crack density.

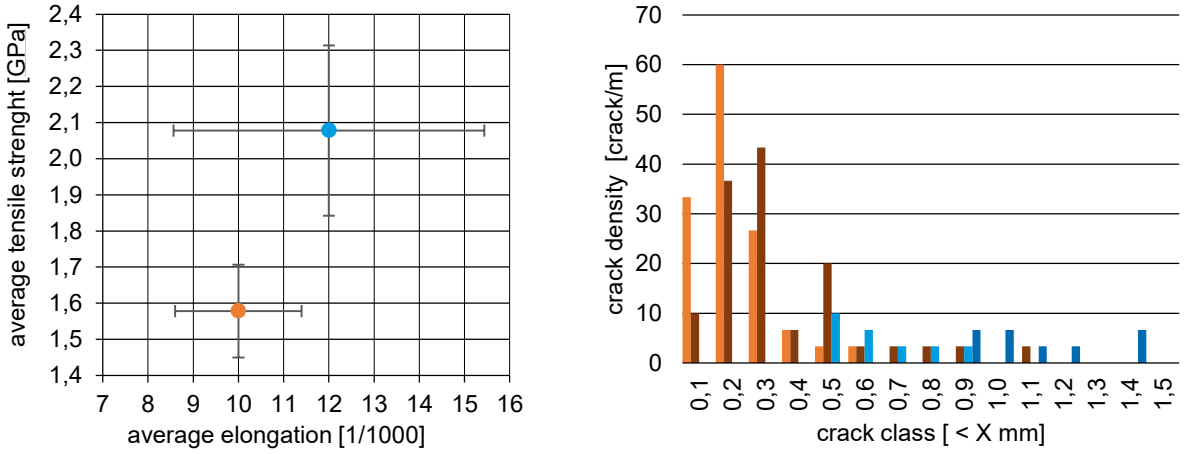

(a)

(b)

Figure 4. (a) Average tensile strength versus average elongation, (b) crack density versus crack width at different strain levels. The crack densities at 50% of the failure strain are shown in light color and at 90% failure strain with brown color. The results of specimens from the online process are shown in orange. The results of conventionally produced specimens are shown in blue.

Figure 4b shows that printed specimens have significantly more cracks with smaller crack widths. At 50% of the failure strain, the majority of the cracks have widths of up to 0.3 mm. Until 90% of the failure strain is reached, the cracks widen uniformly, and an increasing localization of deformation can be observed at one of the cracks. At this crack, tensile fracture of the composite will occur. In contrast, fewer but wider cracks appear in the conventionally

produced specimens. At 50% of the failure strain, there are few cracks with crack widths between 0.5 and 0.8 mm. Up to 90% of the failure strain, there is no further crack formation, but a uniform widening of the cracks. The reason for the greater crack density in specimens from the online process is assumed to be the rougher surface as well as fine cracks forming due to shrinkage. Stress singularities occur at these structural defects and promote crack formation or crack growth. Defects in the concrete resulting from the extrusion process have the same effect.

Visual inspection

The specimens from online and conventional production showed significant differences in failure strength and crack pattern. Imperfections during yarn placement in the online process and imperfections in concrete were assumed to be the main reasons for the differences. Thus, these features were further investigated.

One option to analyze the position of the reinforcements in the specimen is to cut the specimen along longitudinal and transverse directions and measure the position of the yarns. This destructive specimen preparation is very time-consuming when the formation of disturbing artifacts shall be reliably avoided. Furthermore, the image information can only be recorded at one section at a time.

Computed tomography (CT) offers a better alternative for non-destructive as well as three-dimensional imaging of specimen volume. In collaboration with the Institute for Parallel and Distributed Systems, University of Stuttgart, unloaded sections of strain plates (L x W x H = 50 mm x 40 mm x 20 mm) were scanned in a CT. From the data, a digital 3D model of the specimen was generated, in which the embedding of the carbon rovings and the quality of the printed concrete can be analyzed layer by layer. Figure 5 shows a horizontal section and a vertical section of a specimen produced by 3D printing. From the pictures, conclusions can be drawn about the position and orientation as well as the quality of the embedment of the yarns in the concrete.

In Figure 5b it can be clearly seen that all three carbon yarns were displaced from the specimen center, most likely by the volume flow of the concrete during extrusion. The volume flow of concrete from above pushes the yarn downwards. In the case of the central yarn, this displacement is much greater than for the yarns at the edges. A higher position of the yarn supply unit or an adjustment of the printhead nozzle could help to avoid that. It can also be seen that the carbon rovings are not always completely embedded in the concrete. During the printing process, the rovings are supplied with fresh concrete from above, so that air pockets on the underside of the yarns can prevent the formation of a uniform bond. Along the longitudinal axis of a yarn, such bonding defects can be found again and again. Note that an analogous phenomenon can occur in the production of reinforced shotcrete layers. There, an attempt is made to avoid the formation of spray shadows behind the reinforcement by spraying from different angles. In the 3D concrete printing using the method described above, only changes in nozzle geometry or a lower consistency of the fine concrete used can remedy the situation.

Figure 5a shows a longitudinal section of a print specimen. Only two out of three carbon rovings are visible here. The middle roving lies deeper and is not exposed in the selected cut; cf. also Figure 5b. The yarns exhibit slight ondulation and twisting of the filaments in the yarn. These features originate on the one hand from the wrapping of the reinforcement elements with cotton thread and on the other hand from imperfections during yarn placement in the print process. As a result, not all filaments in the yarn are exactly aligned in the direction of tensile loading. With increasing elongation, the filaments are subjected to different levels of stress and fail one after the other. This leads to a lower tensile strength of the entire yarn. However, yarn ondulation as a result of wrapping also offers advantages: Wrapped yarns

show a stronger bonding to concrete, since the latently existing material-chemical bonding components are supplemented by mechanical bonding components, so-called form closure.

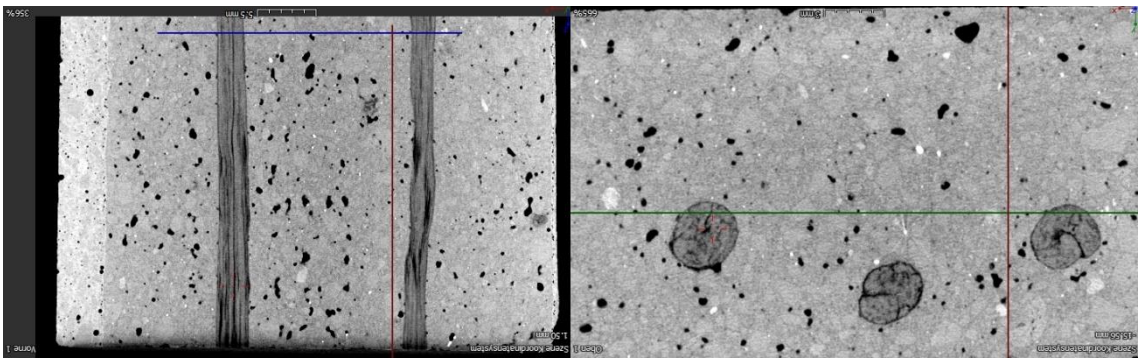

Figure 5. CT Scans of specimen made by online-method: (a) horizontal section, (b) vertical section. The colored lines mark a Cartesian system of coordinates. The sections run through their origin. Scans were made at Institute for Parallel and Distributed Systems, University of Stuttgart.

Downsizing of the concrete filament – fine filament printing

Carbon is a very high-performance material. One disadvantage, however, is that it is more expensive compared to steel reinforcement. It is therefore less suitable as reinforcement for printing solid walls (e.g., with widths ranging from 100 mm to 200 mm), since large quantity of carbonis necessary to achieve a reasonable reinforcement ratio. For this reason, research is being carried out on 3D concrete printing with fine filaments. Here, concrete filament cross-sections of 20 mm by 10 mm with an integrated mineral-impregnated carbon roving shall extruded, while high-strength concrete with a maximum aggregate size of 2 mm is used. Via a mortar pump, the previously mixed fine concrete reaches the nozzle, which is attached to the end of the robot arm. The six-axis robot arm (KUKA) serves as a manipulator and moves the extruder along the previously programmed paths to print the desired elements. The path is calculated by using a 3D-design software Rhinoceros®. The desired geometry is created and translated into the control language of robot by means of Rhinoceros®-plug-in Grasshopper.

The immense degrees of freedom in the movement of extruder through the six axes robot are advantageous. This makes it possible to approach any point in the robot's working area from different directions. This opens up the use of this manufacturing technique for geometrically complex structures such as material minimized shapes, facade elements, but also for complex components with later assembly such as ceiling elements. First examples of such

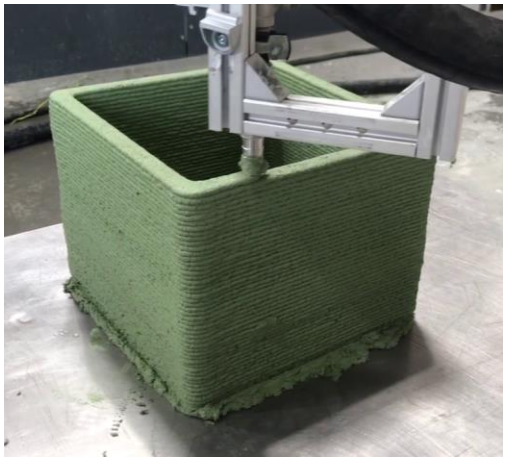

decorative elements can be seen in Figure 6.

Figure 6. Decorative elements from the fine filament 3D concrete printing.

Outlook

In the near future, not only decorative elements but also high-performance load-bearing components will be printed at the Institute for Construction Materials of TU Dresden. The research is performed within the framework of the SFB/TRR280. A particular focus is set on the integration of carbon rovings into the extruded concrete filament. Furthermore, by varying between reinforced and unreinforced concrete filaments, varying reinforcement degree appropriate to the designed load path will be introduced. This in turn leads to cost savings and conserves resources.

For an economical additive construction process, the development of a set on demand system is being implemented as well. Here, the fresh concrete is retarded and thus guarantees a long time in which it can be processed, i.e. pumped and extruded. Once it has been pumped to the nozzle, the concrete is cured in a very short time by adding and mixing in an accelerator. The curing of the concrete filament is controlled, so the printing speed and thus the construction rate can be increased. Rapid stiffening allows any construction height without the risk of collapse or buckling.

Additive manufacturing is becoming more and more important, especially in research but also for innovative companies. With excitement, we can hope for new structures with interesting designs that this new technology will produce.

Data availability statement

Data sharing is not applicable to this article.

Author contributions

Conceptualization, writing—original draft preparation Tobias Neef, writing—review and editing Viktor Mechtcherine. All authors have read and agreed to the published version of the manuscript.

Competing interests

The authors declare no conflict of interest.

Funding

The German Research Foundation (DFG) within the project SFB/TRR280 „Konstruktionsstrategien für materialminimierte Carbonbetonstrukturen – Grundlagen für eine neue Art zu bauen“ funded the research with the project number: 417002380.

References

1. G. De Schutter, K. Lesage, V. Mechtcherine, V. N. Nerella, G. Habert, and I. Agusti-Juan, „Vision of 3D printing with concrete — Technical, economic and environmental potentials“, Cem. Concr. Res., vol. 112, pp. 25–36, 2018, doi: https://doi.org/10.1016/j.cemconres.2018.06.001

2. „3D-Betondruck: Deutschlands erstes Wohnhaus wird gedruckt“. https://www.dabonline.de/2020/11/26/3d-betondruck-deutschlands-erstes-wohnhaus-wird-gedruckt-beckum-beton-peri/. [accessed: Juli 27, 2021]
3. T. A. M. Salet, Z. Y. Ahmed, F. P. Bos, and H. L. M. Laagland, „Design of a 3D printed concrete bridge by testing“, Virtual and Physical Prototyping, vol. 13, no. 3, pp. 222–236, July 2018, doi: https://doi.org/10.1080/17452759.2018.1476064
4. N. Hack and H. Kloft, „Shotcrete 3D Printing Technology for the Fabrication of Slender Fully Reinforced Freeform Concrete Elements with High Surface Quality: A Real-Scale Demonstrator“, in RILEM Bookseries, vol. 28, Springer, 2020, pp. 1128–1137, doi: https://doi.org/10.1007/978-3-030-49916-7_107
5. H. Ogura, V. N. Nerella, and V. Mechtcherine, „Developing and testing of Strain-Hardening Cement-Based Composites (SHCC) in the context of 3D-printing“, Materials (Basel)., vol. 11, no. 8, pp. 1–18, 2018, doi: https://doi.org/10.3390/ma11081375
6. T. Neef, S. Müller, and V. Mechtcherine, „3D-Druck mit Carbonbeton: Technologie und die ersten Untersuchungsergebnisse“, Beton- und Stahlbetonbau, vol. 115, no. 12, pp. 943–951, Dez. 2020, doi: https://onlinelibrary.wiley.com/doi/10.1002/best.202000069
7. V. Mechtcherine et al., „Integrating reinforcement in digital fabrication with concrete: A review and classification framework“, Cem. Concr. Compos., vol. 119, pp. 103964, Feb. 2021, doi: https://doi.org/10.1016/j.cemconcomp.2021.103964
8. K. Schneider, A. Michel, M. Liebscher, L. Terreri, S. Hempel, and V. Mechtcherine, „Mineral-impregnated carbon fibre reinforcement for high temperature resistance of thin-walled concrete structures“, Cem. Concr. Compos., vol. 97, pp. 68–77, March 2019, doi: https://doi.org/10.1016/j.cemconcomp.2018.12.006
9. V. Mechtcherine, A. Michel, M. Liebscher, K. Schneider, and C. Großmann, „Mineral-impregnated carbon fiber composites as novel reinforcement for concrete construction: Material and automation perspectives“, Autom. Constr., vol. 110, pp. 103002, 2020, doi: https://doi.org/10.1016/j.autcon.2019.103002
10. V. Mechtcherine, A. Michel, M. Liebscher, and T. Schmeier, „Extrusion-based additive manufacturing with carbon reinforced concrete: Concept and feasibility study“, Materials (Basel), vol. 13, no. 11, 2020, doi: https://doi.org/10.3390/ma13112568
11. V. N. Nerella, S. Hempel, and V. Mechtcherine, „Effects of layer-interface properties on mechanical performance of concrete elements produced by extrusion-based 3D-printing“, Constr. Build. Mater., vol. 205, pp. 586–601, 2019, doi: https://doi.org/10.1016/j.conbuildmat.2019.01.235
12. V. N. Nerella, M. Näther, A. Iqbal, M. Butler, and V. Mechtcherine, „Inline quantification of extrudability of cementitious materials for digital construction“, Cem. Concr. Compos., vol. 95, pp. 260–270, 2019 doi: https://doi.org/10.1016/j.cemconcomp.2018.09.015